



ELSEVIER

Thermochimica Acta 269/270 (1995) 159–184

thermochimica
acta

Some aspects of thermal effects and application properties of engineering plastics and rubber [☆]

Heinz Moehler

*Polytechnic (Fachhochschule) of Wuerzburg, Department of Plastics and Rubber Engineering,
Roentgenring 8, D-97070 Wuerzburg, Bavaria, Germany*

Received 16 September 1994; accepted 7 February 1995

Abstract

The investigations presented here were made over the last few years at the department of Plastics and Rubber Engineering at the Polytechnic of Wuerzburg/Germany, exclusively in cooperation with German plastic and rubber processing or industrial applications companies. Practical aspects rather than basic research were stressed, e.g. faster characterization of material, characteristics of the final product, optimization of processing processes. Aspects of recycling, of growing importance today, were also considered.

Keywords: DSC; Plastic; Rubber; Thermosetting

1. High-performance plastics

1.1. Non-reinforced and carbon-fibre-(CF)-reinforced thermosets

1.1.1. Kinetic studies on epoxy (EP) resin systems based on differential scanning calorimetry (DSC) measurements [1]

Introduction. Increasingly, aluminium alloys are substituted by fibre composite materials in the aircraft and aerospace industries. They excel because of their low weight at high strengths. However, thermoset matrix materials require long curing cycles during production and also extensive production planning. The matrices of the high-perform-

[☆] Presented at the 6th European Symposium on Thermal Analysis and Calorimetry, Grado, Italy, 11–16 September 1994.

Table 1
Investigated systems and curing parameters

Trade name/ Supplier	Chemical description of the matrix resin	Investigated sample/mixing ratios	Curing temperature/°C	Curing time/ min	Application
Araldit F	Liquid EP resin based on bisphenole A and epichlorohydrine	3-Component resin 100:90:0.5	95	30 60 90	Resin for casting and impregnating in the electro-industry
HY 917	Liquid hardener based on aromatic dicarboxylic acid anhydride				
DY 062	Liquid tertiary amine accelerator				
Ciba-Geigy					
Hysol EA 9390	Tri- and tetra-functional EP resin	2-Component resin	95	60 120 240 480	Low-temperature repair system
Dexter Aero- space Materials		100:56			
Hysol Aero- space Products	Cycloaliphatic tetrafunctional amine hardener				
Fibredux 914C	Multifunctional aromatic EP resin with flow help	CF fabric prepreg with a resin content of 42%	120 180 190	180 120 240	Common prepreg for primary aircraft components, e.g. for the Tornado fighter
Ciba-Geigy	High functional aliphatic hardener				
Hexel X 3100	Multifunctional EP resin with an amine hardener	CF unidirectional (UD) prepreg with a resin content of 40%	83 94 98	60 120 1440	Low-temperature repair prepreg
Hexel Corp.					
Vicotex M18	Unknown EP resin with flow help	Available in a wide range of	120 150	120 120	Newly designed HT and damage

BrochierSA/ Ciba-Geigy Composites	High functional aromatic amine hardener	fabrics, UD tapes and single tows Only the resin film was investigated	180	120	tolerant 180°C EP resin for primary aircraft components with especially low moisture pick-up level, e.g. planned for the Tiger helicopter
-----------------------------------------	-----------------------------------------------	----------------------------------------------------------------------------------------	-----	-----	-------------------------------------------------------------------------------------------------------------------------------------------------------------------

Table 2
Araldite system at a curing temperature of 95°C for two insignificantly (*F*-test) distinguishable three-step follow-on models

Model ^a	Correlation coefficient	F_{exp}	F_{crit}	Curing time/min	Degrees of conversion %		Residual reaction heat method
					MultiScan method	ASTM E 698	
1st O + autocat/1st O/ <i>n</i> th O	0.999984	1.00	1.29	30	43	16	14
				60	80	33	28
				90	92	49	49
<i>n</i> th O/ <i>n</i> th O/ <i>n</i> th O	0.999984	1.01	1.29	30	25	16	14
				60	54	33	28
				90	68	49	49

^aTypes of reaction: 1st O, first-order reaction; *n*th O, *n*th-order reaction; 1st O + autocat, first-order reaction with autocatalysis.

ance fibre composites used in practice are generally chemically crosslinked thermosets (EP resins, poly-imide (PI) resins, etc.), although high-temperature resistant (HT) thermoplastic materials are also being intensively investigated. Many tests with prototypes for optimizing the curing cycles still have to be made because the selection of process parameters, such as temperature, pressure, and viscosity, especially for complex parts or hybrid materials, leave only a small window open for the processor. To save development and production times and production costs, optimizing the curing process parameters by simulation is required. In addition to the reaction kinetic models based on DSC measurements, curing processes must be optimized by considering diffusion and heat transfer processes as well as the rheology in the simulation. But this will not to be discussed here. The systems investigated are listed in Table 1. The kinetic evaluations were made by the NETZSCH MultipleScan multistep kinetics [2,3] and according to ASTM E 698 [4]. In addition, degrees of conversion (curing, crosslinking) were determined by the residual heat method.

Results. Fig. 1 shows the typical shape of the DSC reaction curves for all systems investigated, except the fibredux system, and their shift towards higher temperatures with increasing heating rate (5, 10, and $20^{\circ}\text{C min}^{-1}$) is shown for the Araldit system. It is evident that neither the reaction heat values, $319 \pm 11.8 \text{ J g}^{-1}$ corresponding to a standard deviation of $\pm 3.7\%$ which is quite acceptable for such measurements, nor the peak heights, $0.177 \pm 0.006 \text{ W g}^{-1}$ corresponding to $\pm 3.3\%$, show a significant dependence on the heating rate so that no competing or parallel reactions need be assumed for the kinetic model. During a second heating process, after a controlled cooling, of $40^{\circ}\text{C min}^{-1}$, no exothermicity is observed. The weight losses after the second heating were less than 5%. The glass transition temperature at $101.5 \pm 1.0^{\circ}\text{C}$ is also independent of the heating rate. This means that the curing of the samples, according to the DSC results, is completed after the first heating, regardless of the heating rate. Whether this is absolutely true would have to be checked by long-term curing because, according to the manufacturer, the glass transition of the fully crosslinked Araldit system should be at about 120°C . Therefore, except for the fibredux system whose DSC reaction curve is shown in Fig. 2 together with the second heating both kinetics used in this study should lead to similar results. But despite the unstructured DSC curves of the Araldit system, the best fit with the experimental data was reached by a three-step follow-on reaction model (Fig. 3). Therefore, the differences between the degrees of conversion calculated by both kinetic methods and by the residual reaction heat method are not surprising (Table 2). Similar results were found for all other systems (Table 3).

Conclusions. Comparing the results for the 5 investigated systems (Table 3), the following conclusions can be drawn.

1. None of the systems could be described by a single-step reaction of 1st order, e.g. according to ASTM E 698 when including the full DSC reaction peaks, but this was possible using MultipleScan kinetics even within the conversion range of 2–98% for each DSC curve. In addition, one should remember that ASTM E 698 uses only

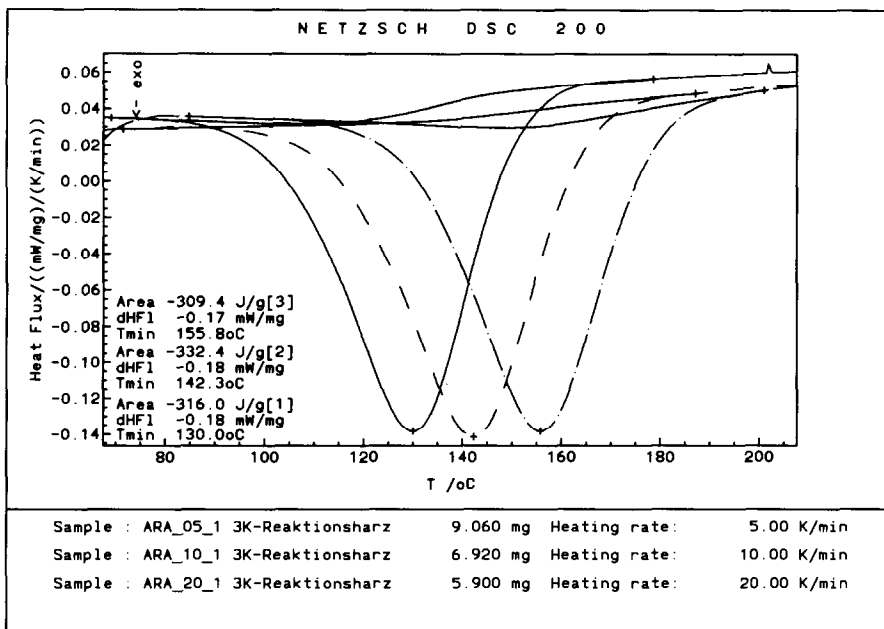


Fig. 1. 1st heating DSC curves of the Araldit F system with heating rates of 5, 10 and 20°C min⁻¹, from left to right.

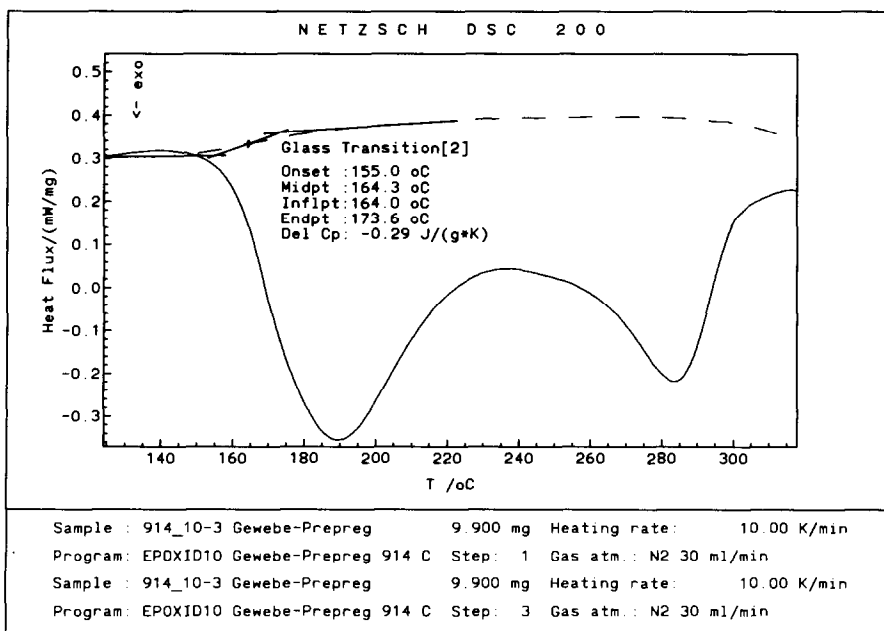


Fig. 2. First (—) and second (---) heating DSC curves of the Fibredux 914 system with a rate of 10°C min⁻¹.

NETZSCH THERMOKINETIC ANALYSIS PROGRAM multiple scan
 NON-LINEAR REGRESSION Date: 24.10.1994
 Problem: ARA F/917/DY062
 Model: 1st ord. with autocat. B A $\xrightarrow{1}$ B $\xrightarrow{2}$ C $\xrightarrow{3}$ D
 f: 1st order
 f: n-th order

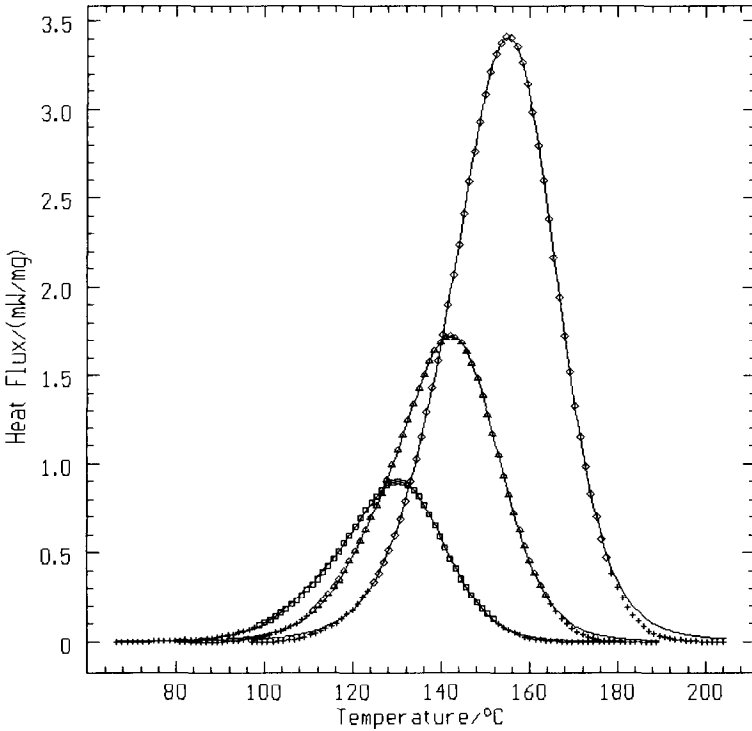


Fig. 3. Best MultiScan curve fits (solid curves) of the DSC reaction curves of Fig. 1 realized by a triple-step follow-on reaction.

discrete points of the reaction curve. This procedure was suggested by Carpenter [5] and applied in this investigation.

2. The degree of conversion evaluated by residual heat measurements as a dimension for the degree of cross-linking is only permissible for single-step reactions and/or if the reaction heats of the intermediate stages are negligible in contrast to the network-forming step, which can certainly not be assumed.
3. For comparing degrees of crosslinking, or better the relative degrees of network density, with reaction kinetic evaluations of DSC MultipleScan measurements, mechanical properties such as the interlaminar shear strength (ILSS) are the best, as shown in Fig. 4. But one should remember that ILSS [6, 7], as compared to DSC, is a very time- and manpower-consuming method.

Table 3
Summarized comparison with regard to the best MultiScan modelling results according to *F*-tests and correlation coefficients

Trade name/ Supplier/Other features	Curing temp./ °C	Curing time/min	MultiScan modelling		Degrees of conversion %		Application possibilities	
			Model	Correlation coefficient	Degrees of conversion %	Residual reaction heat method		ASTM E 698
Araldite F/HY917/ DY 062 from Ciba- Geigy with a mixing ratio of 100:90:0.5	95	30	1st O + autocat/1st O/nth O	0.99998	43	14	16	Resin for lamination
	95	60			80	28	33	
	95	90			92	49	49	
Hysol EA 9300 with a mixing ratio for the components A:B of 100:56 from Dexter Aerospace Materials Division, Hysol Aerospace Products	95	60	1st O + autocat/1st O/nth O	0.99989	96	91	100	Low-temperature 2-component repair adhesive
	95	120			100	90	100	
	95	240			100	90-92	100	
	95	480			100	93	100	
Fibredux 914 CF prepreg with 42% resin content from Ciba-Geigy	120	180	1st O/1st O/ nth/O	0.99417	0	35	36	Common prepreg system for primary structures used, e.g., for the Tornado fighter
	180	120			28	80-85	100	Low-temperature prepreg-system for repair
	190	240			81	100	100	Newly designed prepreg system for primary structures, e.g. planned for the helicopter Tiger
Hexol X 3100, CF UD-prepregs with 40% resin content from Hexel Corp.	83	60	1st O/1st O/ 1st O + autocat	0.99740	18	18	73	
	94	130			98	80	100	
	98	1440			100	80-90	100	
Vicotex SXM18 CF pre- pregs with variable setup and 32 % resin content from Brochier S.A. Ciba-Geigy Compo- sites. Only the resin film was investigated	120	120	nth O/nth O/ nth O	0.99983	12	22	46	
	150	120			72	87	100	
	180	120			83	98	100	

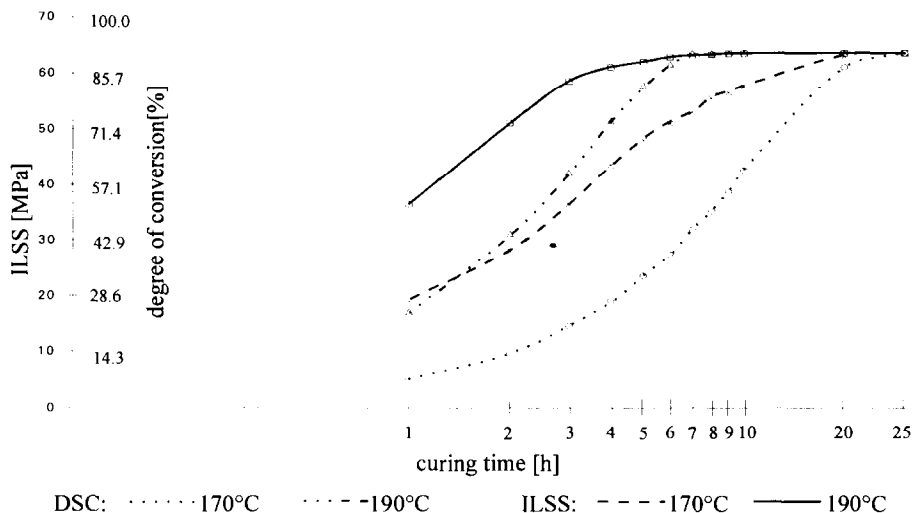


Fig. 4. Interlaminar shear strength and the degree of conversion of the Fibredux 914 C system calculated from MultiScan modelling of a triple-step follow-on reaction based on DSC curves with heating rates of 5, 10 and 20°C min⁻¹.

- Furthermore, the occurrence of negative shares of reaction steps in the MultiScan multistep model indicates that exothermal and endothermal reaction steps are superimposed within the entire reaction, that the measured reaction heat cannot correspond to the degree of conversion, and that the degree of conversion obtained by the multistep model must be higher than those obtained from the residual heat method or according to ASTM E 698 [8].

In conclusion, while considering only the best model calculated by the MultiScan multistep method within a conversion range of 0.02–0.98, the differences relative to the residual heat method and the single-step 1st-order reaction according to ASTM E 698 become evident because of the weak points of these two methods mentioned previously.

1.1.2. Influence of prepreg storage and laminate conditioning on the viscoelastic properties and the glass transition temperatures of EP- and PI/CF-laminates

The dynamic mechanical properties of these laminates are drastically influenced by prepreg storage and laminate conditioning, especially under humidity [9]. For this purpose, 8-layer EP/CF-laminates with a layer order of (0/45/-45/90)s were made from UD prepreps of a thickness of about 200 μm (trade name; Vicotex R 6376/40%/G 814 of Brochier S.A/Ciba-Geigy) with a resin content of 40%, and investigated by dynamic mechanical analysis (DMA) in the 3-point bending mode. This corresponds to an effective fibre content F of 60% parallel to the long sample axis of the laminates.

The prepreps were stored for 0, 250 and 500 h at 23°C and 50% relative humidity. The laminates were produced in an autoclave according to the specification of the manufacturer [10]. Then, a portion of each laminate was conditioned for about 7 weeks

at 70°C in vacuum until a constant weight was reached, and another portion at 40°C in a water bath. Fig. 5 shows the DMA curves of a laminate after vacuum drying without prepreg prestorage. The solid curve shows the storage modulus, the dash-dotted one the loss modulus and the dashed one the loss factor as a function of the temperature for a testing frequency of 1 Hz, a target deformation amplitude of $\pm 30 \mu\text{m}$ and a heating rate of 3°C min^{-1} , measured in a temperature range of -60 to $+320^\circ\text{C}$. The effective sample dimensions were 40 mm in length, 9.97 ± 0.05 mm in width, and 1.78 ± 0.18 mm in thickness. The results are shown in Table 4. There is a striking decrease in the glass transition temperatures after water storage compared to the vacuum drying process, although this is a system optimized for a very low absorption of humidity [10]. Another interesting feature is the steps in the pattern of the storage modulus, at 267°C for the dry system and at 273.3°C for the system saturated with humidity. In addition, the wet system shows a step in the $\tan \delta$ curve at about 195°C . Keeping in mind all these results as a function of prepreg storage at 23°C and 50% relative humidity, it can be seen that the characteristic temperatures and the appropriate storage moduli change significantly especially in the 2nd onset and/or in the $\tan \delta$ maxima. It must also be said that the storage moduli adjust to one another during the 500 h of storage. The same is true of the $\tan \delta$ values, although not to such a high degree. This indicates a certain dehydration of the parts saturated with humidity and a certain absorption of humidity during prepreg storage of the dried samples. The glass transition temperatures T_g , however, are

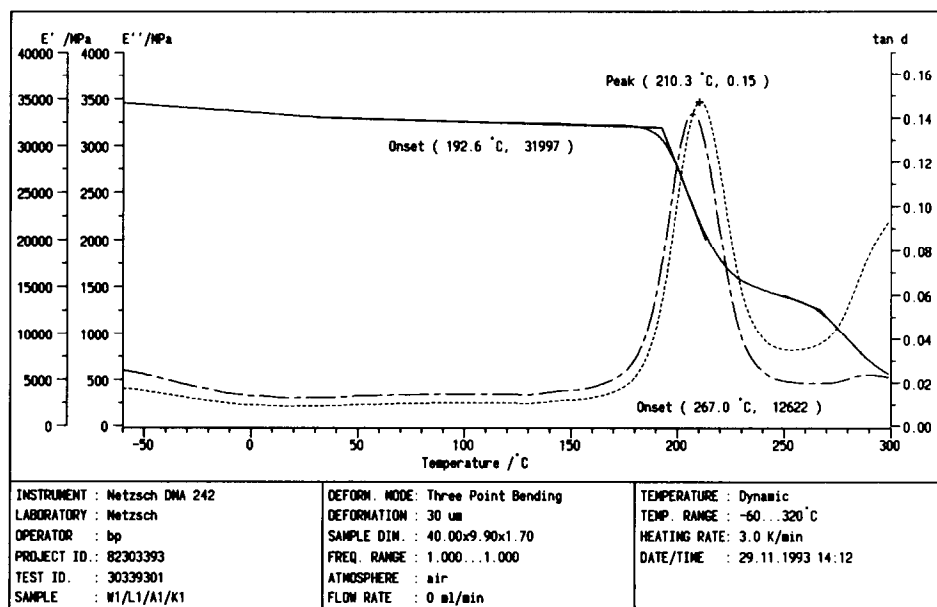


Fig. 5. DMA spectrum (storage modulus (—), loss modulus (— · — · —) and loss factor, $\tan \delta$ (----)) of a (0/45/-45/90)s EP/CF laminate made of Vicotex R 6376/40%/G814 UD prepreps after vacuum drying at 70°C without prepreg prestorage.

Table 4

Influence of laminate conditioning and prepreg storage at 23°C and 50% relative humidity on the viscoelastic properties of EP/CF laminate

Laminate conditioning	Prepreg storage at 23°C and 50% r.h./h	Storage modulus				tan δ (T_g) Maximum		Remarks ^c
		1st onset (T_g)		2nd onset ^a		°C	Value	
		°C	GPa	°C	GPa ^b			
7 Weeks vacuum drying at 70°	0	192.6	32.0	267.0	12.6	210.3	0.147	
	250	194.7	29.8	274.2	14.6	210.9	0.122	
	500	193.4	34.2	270.7	16.8	211.7	0.104	
7 Weeks water storage at 40°C	0	146.8	32.0	273.3	12.6	162.8	0.089	200°C
	250	144.4	31.3	262.6	13.3	161.8	0.089	200°C
	500	141.2	34.3	259.6	15.3	160.8	0.082	195°C

^a Step due to softening of the sample during post-curing (DSC measurements).

^b Due to storage conditions.

^c tan δ shoulder.

strongly influenced so that the permanent application temperature has probably to be restricted to 140°C under such extreme conditions. Up to this temperature, the material obviously tolerates considerable differences in humidity in its environment.

Similar results were obtained by TMA measurements (Dilatometer 402 ET, Netzsch-Gerätebau) of EP/CF and polyimide (PI)/CF laminates [11]. Both laminates were produced in an autoclave from 32 125 μm thick UD EP-prepreg layers (trade name: Fiberite E 1076 E of Dornier GmbH) with a resin content of 34–40%, as UD laminates and multidirectional (MD) laminates with a layer order of (45/90/-45/0/0/-45/90/45)2 s, and from 26 125 μm thick UD PI-Roving prepreg layers (trade name: Sigrafil CI-1020 of Sigril Great Lakes Carbon GmbH; formerly Sigril GmbH) with a resin content of 33–37%, also as UD laminates and MD laminates with a layer order of [0(0/45/-45/0)3]s. The EP resin is probably a polyfunctional resin (maybe tetraglycidylmethylenedianiline, TGDMA) with an aromatic diamine (maybe diaminediphenylsulphone, DDS) and the PI resin is probably a bismaleinimide with a diaminediphenylmethane hardener. Samples of size 20 \times 8 mm² were cut from laminate plates of dimensions 300 \times 300 mm² using a diamond-impregnated separating wheel under water cooling. The measurements took place immediately after storage with a heating rate of 5°C min⁻¹. The length of the samples was 20 mm.

Table 5 shows the results for both matrices. Surprisingly, no reproducible results could be obtained for high effective fibre contents in the measuring directions. Microscopic inspections showed delaminations in the direction of the 0° fibre orientation caused by the sample preparation (drying and storage in humidity). This explains the non-reproducible results for the high effective fibre contents F of 86 or 100%. It is striking for both matrix resins how the glass transition temperature decreased con-

Table 5
TMA results

Sample size in mm ² /laminate type	Conditioning	EP/CF laminates			PI/CF laminates	
		F%	T _g /°C with 99% range of confidence	Starting temperature of post-curing with 99% range of confidence	F%	T _g /°C with 99% range of confidence
20 × 8/UD	Dry	100	n.r.	n.r.	100	n.r.
	70°C/75% r.h.		n.r.	n.r.		n.r.
	70°C/95% r.h.		n.r.	n.r.		n.r.
20 × 8/UD	Dry	0	208.5 ± 3.2	237.9 ± 2.0	0	289.4 ± 5.6
	70°C/75% r.h.		125.5 ± 7.3	186.0 ± 7.5		149.5 ± 6.4
	70°C/95% r.h.		103.0 ± 2.1	177.7 ± 3.5		125.2 ± 7.9
20 × 8/MD parallel to 0° fibre	Dry	60	216.7 ± 4.1	227.7 ± 3.0	86	n.r.
	70°C/75% r.h.		143.1 ± 12.7	175.4 ± 7.2		n.r.
	70°C/95% r.h.		126.1 ± 15.6	157.9 ± 16.1		n.r.
20 × 8/MD perpendicular to 0° fibre	Dry	60	217.9 ± 2.9	230 ± 6.3	33	303.3 ± 14.3
	70°C/75% r.h.		146.3 ± 11.9	174.7 ± 7.0		154.5 ± 10.8
	70°C/95% r.h.		123.2 ± 5.1	158.2 ± 5.1		141.5 ± 7.0

Key: r.h., relative humidity; n.r., non-reproducible results.

siderably on absorption of humidity. It is considerably higher than that of Vicotex R 6376/40%/G 814 EP/CF laminates, caused by the considerably higher humidity absorption of the matrix resins. This explains, of course, the extreme decrease of the glass transition temperature for a fibre content of 0% in the measuring direction.

1.2. Electron-beam-crosslinked polyamide 66 for applications in the electronic industry [12]

For reasons of economic and application properties, the electronic industry, in contrast to the automotive industry where reactive compounding is of top interest, especially for thick-walled parts, prefers electron-beam crosslinking over chemical crosslinking. In many cases, this technology offers to replace very expensive and hard-to-process materials like PEEK by cheaper polymers like polyamide which are easy to process. Unfortunately, until now, there has been practically no information available concerning the electron-beam crosslinking of PA66. Therefore, Ultramid A3X165 nf of BASF AG, an important material for functional parts like contactors, was investigated here because if electric arcs develop at the moment of switching, the parts are subjected to temperatures up to 430°C. However, the melting point of non-crosslinked PA66 is only 255°C. So mobile parts of the contactors may melt so that contact carriers or slides will jam and the function of the contactor is no longer ensured.

But it was thought that it would not be affected when those parts of the contactor are made of crosslinked material and that the required properties would only be achieved and maintained when a sufficient quantity of crosslinking material like triallyl-isocyanurate (TAIC) is added to the granulate. In this investigation, Betalink IC/W70 (trade name of Plastic-Technology-Service, Tauberzell, Germany), with a nominal TAIC content of 70 mass%, was used as a crosslinking agent. Using thermogravimetry (TGA), a value of 67.8 ± 0.2 mass% was measured. In order to facilitate the handling, Betalink contains calcium silicate as a carrier. The next step was to find suitable inspection methods for the individual processing steps.

Mixing step (adsorption of Betalink by the polymer). First the polyamide was dried at a processing humidity of less than 0.2%. Then 1–6 mass% of Betalink was added and the amount adsorbed by the polymer during mixing was determined. Mixing took place in a tumbling mixer at a speed of 60 r.p.m. for 15–20 min. The warm granulate adsorbs the crosslinking agent up to 4 mass% so that it can practically no longer be seen after mixing. This procedure can readily be checked with a balance, especially if one works discontinuously in batch operation.

Injection moulding step (weight loss during injection moulding). Considering the fact that Betalink shows a weight loss starting at about 100°C, a loss of crosslinking agent must be expected during injection moulding. Injection moulding took place on an all-rounder 270-90-350 (Arburg, Loßburg/Germany). Because the viscosity of the batch is reduced by adding the crosslinking agent, cylinder and nozzle temperature had to be reduced by 10°C from an addition of 5 mass% Betalink on. With 4 mass%, the temperature of the feeding zone was 60°C and both the cylinder temperature in all three zones and the nozzle temperature were 280°C. The mould temperature was 80°C. All the other injection moulding parameters were kept constant. TGA turned out to be the suitable method using the following program: sample mass, about 6.5 mg; purge gas and rate, nitrogen at 60 ml mm⁻¹; heating up from 50°C at 10°C min⁻¹ to 80°C, holding for 5 min, and heating up again at 10°C min⁻¹ to 200°C, and holding again for 10 min.

Approximately 40 min are required for one measurement. To reach the highest possible specific surface, the samples were carefully (avoiding heating) filed off from the injection-moulded parts. So the mass loss between 80 and 200°C including the isothermal holding turned out to be a suitable parameter for the characterization of the influence of the injection moulding step (Fig. 6, dash-dotted line). The blank value of the polyamide without the cross-linking agent was of course taken into consideration. It was independent of the crosslinking-agent content at the crosslinked material somewhat higher than at the non-crosslinked polyamide. This can be explained by polymer degradation by β -irradiation and, possibly, the slight residue of TAIC. The standard deviations of $\pm 7.5\%$ for 1% Betalink and $\pm 2.6\%$ for 6% Betalink determined in 9 single measurements do not indicate accidental inhomogeneity of the samples regarding a sample mass of about 6.5 mg. On the basis of the TGA results, the weight loss of 2 g samples held for 60 min at 200°C in an oven was determined. Fig. 6 (solid line) shows a good correlation between TGA and oven values.

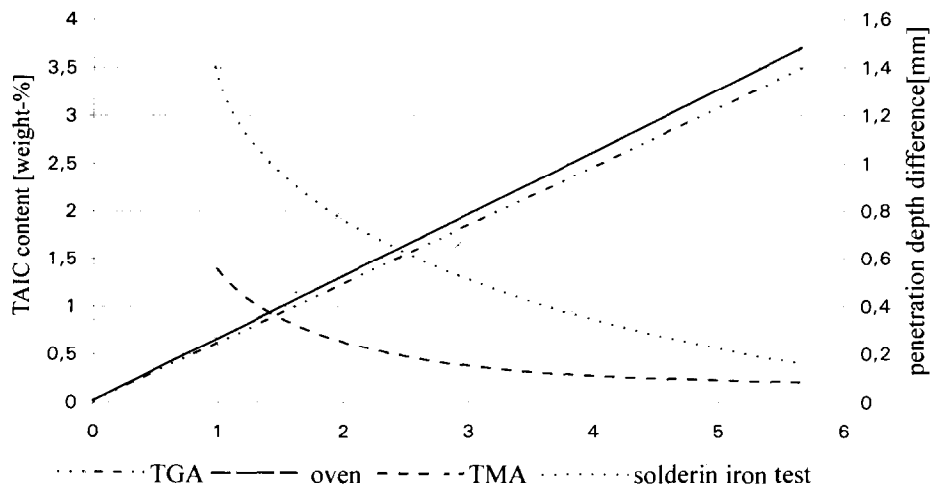


Fig. 6. Triallylisocyanurate (TAIC) content after injection moulding (TGA and oven storage) and after electron-beam crosslinking (TMA and soldering iron test).

This means that only an oven is needed at the injection moulders to monitor this production step.

Influence of crosslinking. The crosslinking took place in a 4.5 MeV electron beam accelerator. 1000 kGy ($1 \text{ Gy} = 1 \text{ J kg}^{-1}$) is regarded as the optimal beam dosage for polyamide without crosslinking agent [13]. With Betalink, we found by extraction measurements that 100 kGy are enough. Since mechanical methods such as tensile strength are very time-consuming, especially when the temperature dependence is of interest, as is the case here, dilatometric penetration measurements were carried out based on the determination of the Vicat softening temperature. The hemispherical pin (radius, 0.5 mm; height, 2 mm) of a penetration sample probe was loaded with 100 g and then the following program was run:

Heating at $10^\circ\text{C min}^{-1}$ from 200 to 270°C followed by 10 min isothermal holding. The difference in the penetration depths in the isothermal part of the penetration curve at 270°C between 2 and 10 min was defined as the suitable parameter. A clear correlation between the adsorbed Betalink content and the penetration value which characterizes the crosslinking density is apparent up to 4% Betalink (Fig. 6, dashed line). On the basis of these results, a soldering iron penetration tester was developed which can be used simply on the production line. These results are also entered in Fig. 6 (dotted line) with a temperature of about 340°C for the penetration pin, a load of 22 N and a penetration time of 10 s. Furthermore, it could be shown by gel permeation chromatography that the medium mol mass of the soluble share of the crosslinked samples decreased when the crosslinking agent increased, which means that there is a correlation between mol mass decrease and the inverse penetration depth.

2. Blends and copolymers

Impact-modified polypropylene blends and polypropylene/polyethylene block copolymers are becoming very important materials for automobile applications, especially because of their favourable cost-performance ratio and their good recycling properties [14].

Therefore the target of this study was to establish a correlation between the time-consuming impact strength measurements by instrumental puncture tests, according to DIN 53 443, and values determined considerably more quickly by DMA within the glass transition range of the impact-modifying EPM component around -60°C . Table 6 lists the investigated materials, which differ with respect to their type (blend or block copolymer) as well as their softphase content and the surface structure of the injection-moulded parts. The blends are so-called reactor blends.

In addition to the results of the instrumental puncture and the DMA tests, DSC and melt-flow-index (MFI) measurements were carried out. The results are summarized in Table 7 and compared with the data given by the raw material manufacturers. The reasons for the deviations between the manufacturer's data and the values calculated from the DSC measurements, as observed in part for the soft phase, is probably due to the separation of the superimposing PE and PP melt peaks (only partial area integration but no peak separation software was available), difficulties in the definition

Table 6
Investigated plastics

No.	Trade name (colour)	PP grade	Number of samples	Remarks
1	Hostacom X 678/1 (brown)	Blend	50	Smooth surface 20% talcum
2	Hostalen PPN 1034 (natural)	Block copolymer	100	Smooth surface non-reinforced
3	Hostalen PPR 1042 (black)	Block copolymer	50	Smooth surface non-reinforced
4	Hostacom X 4305 (black)	Block copolymer	44	Smooth surface 20% talcum
5	Hostalen PPT 8009 (black)	Blend	100	Scarred surface ^b non-reinforced
6	Hostalen PPR 8008 (black)	Blend	100	Scarred surface ^b non-reinforced
7	Hostalen PPX 4201 ^a (black)	Blend	100	Scarred surface ^b non-reinforced
8	Hostalen PPN 8018/B (beige)	Blend	20	Smooth surface non-reinforced
9	Hostalen PPN 8009 (black)	Blend	20	Smooth surface non-reinforced

^a Incomplete supplier data (experimental stage product).

^b Only one surface of the sample.

Table 7
MFI and composition of the blends/copolymers

No.	MFI results/(g/10 min)		Weight% calculated from DSC measurements			Weight% softphase ^d
	Measured values	Values given by the supplier ^c	PE	PP	EPM	
1	4.3 ± 0.12	4.5	1.7	66.7	11.6 ^d	8–10
2	2.5 ± 0.09	1.5	3.8	84.6	11.6	12–15
3	5.3 ± 0.18	4.0	4.2	83.9	11.9	13–17
4	12.6 ± 0.69	16.0	0	74.2	5.8 ^d	17–20
5	3.6 ± 0.15	5–8.5 ^a	16.9	43.1	40.0	28–30
6	4.8 ± 0.15	3–4 ^a	11.5	52.6	36.9	40–45
7	7.7 ± 0.33	– ^b	14.0	33.7	52.3	45–50
8	3.3 ± 0.14	1.4–2 ^b	15.6	60.7	23.7	45–50
9	1.4 ± 0.05	2.0	16.2	40.4	43.4	45–50

^a MFI 190/21.6.

^b No supplier values available (experimental stage product).

^c Hostalen PP leaflet.

^d 20% talcum reinforced.

of the base line especially at very low PE contents, and the empirical equation for the evaluation of the PE content, which is only valid up to a PE content of approx. 20% [15].

Because the soft phase content stated by the manufacturer is made up of EPM and PE, these two values have to be added to Table 7 in order to be comparable with the manufacturer's data. One of the most interesting properties regarding exterior plastics parts in car manufacture is the low temperature flexibility at impact stress. The energy absorbed by the sample at the glass transition temperature and a puncture speed of 4.43 m s⁻¹ is considered to be a standard test method for estimating the tough/brittle behaviour of plastics exposed to impact stress. Starting at room temperature, the temperature was raised or lowered in steps of 5°C until the transition temperature of the tough/brittle zone was determined. Three samples per material were punctured at each temperature. As this test procedure requires a lot of time and equipment, other methods were looked for. DMA seemed to be a suitable alternative. Fig. 7 shows a typical three-point bending DMA spectrum of the investigated blends with the shift of the glass transition temperatures characterized by the onset temperatures of the storage modulus and the peak temperatures of the loss factor tan δ for five frequencies between 1 and 20 Hz and a heating rate of 3°C min⁻¹. The values for the three phases of the blend at 1 Hz were calculated with -140.8°C for the onset and -131.7°C for the tan δ peak of the polyethylene component, with -65.6 and -55.7°C for the EPM component, and -3.7 and 13.0°C of the polypropylene component. Using the Arrhenius equation, which was not done here, one can also calculate the glass transition temperatures at application frequencies that cannot be reached by the DMA spec-

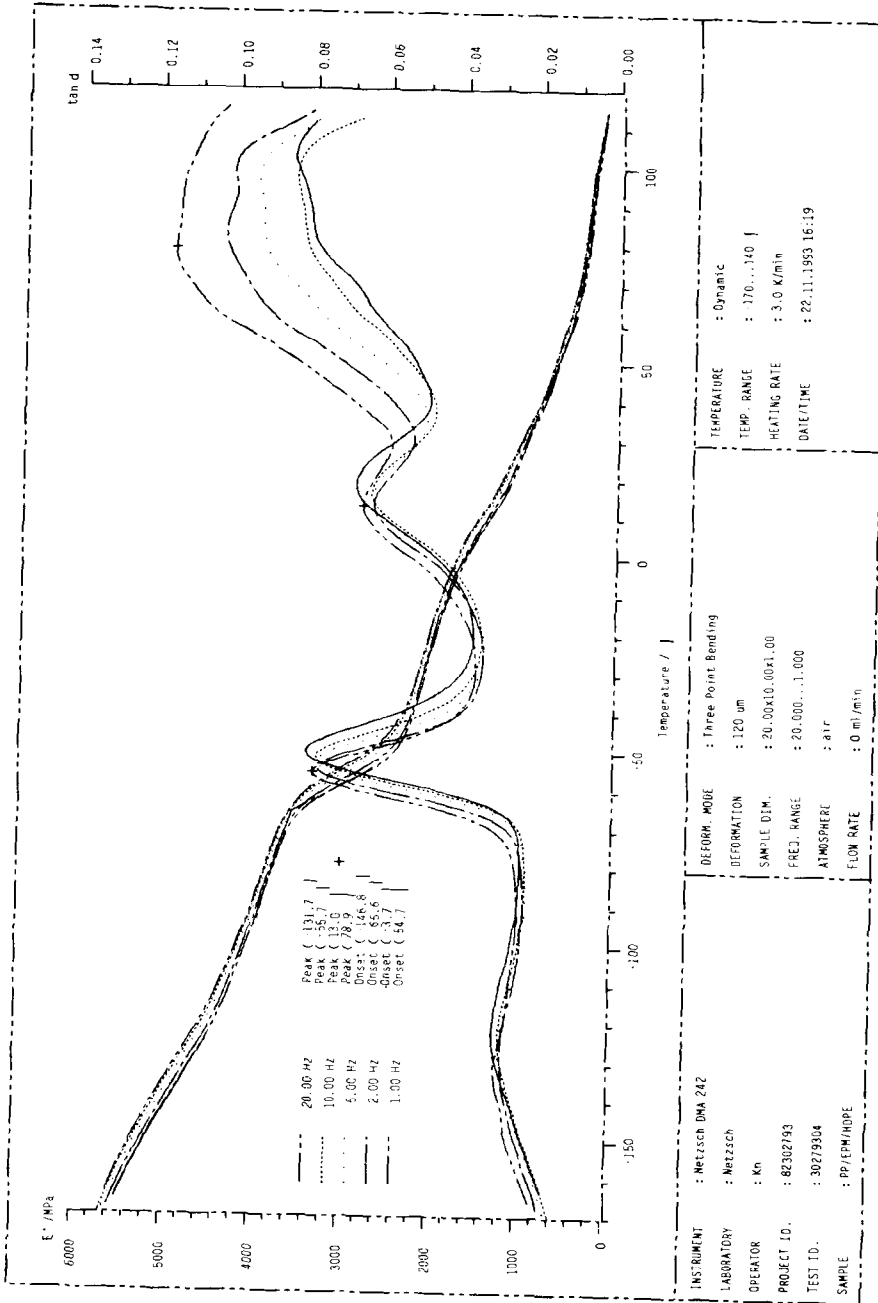


Fig. 7. Typical three-point bending DMA spectrum of the storage moduli and the loss factors $\tan \delta$ of an elastomer modified blend from Table 6 measured at frequencies of 1, 2, 5, 10 and 20 Hz and a heating rate of 3°C min^{-1} .

trometer. This is also very important for application of finished plastic parts, for example in the automotive industry. Since it can be assumed that the EPM component is mainly responsible for the low-temperature flexibility, the peak height $\Delta \tan \delta$ and the peak area were evaluated. Taking into consideration that the transition temperatures from the puncture tests were determined in steps of 5°C , satisfactory correlations between the soft phase contents determined by DSC as well as the peak heights $\tan \delta \Delta$ of the EPM peaks and the transition temperatures could be established for the unfilled as well as for the talcum-filled blends and block copolymers, with the exception of one polymer blend (material no. 6) (Fig. 8). The expected strong influence of talcum is striking. Surprisingly, greater uncertainty is to be observed with the area evaluation than the peak height evaluation. To sum up, it can undoubtedly be said that DSC and also DMA appear to be suitable for distinguishing elastomer-modified PP blends with respect to their low-temperature flexibility. These investigations are being continued, particularly in view of the influence of the surface structure on the transition zone determined with the puncture test, especially since no strong deviations occur when grained materials are left out.

In this context, the presentation of studies on the anisotropy of self-reinforcing liquid crystalline polymer blends for injection moulding [16] or on the optimization of the heat stability of thermoplastic elastomers based on urethane by means of blending with thermoplastics such as polybutylene terephthalate, polyphenylene sulphide or aromatic polyester carbonate, or of thermoplastic elastomers which are based on ether or ether ester amide [17], is also of interest from the scientific point of view. These materials are not yet in general use, so they will not be discussed in this article.

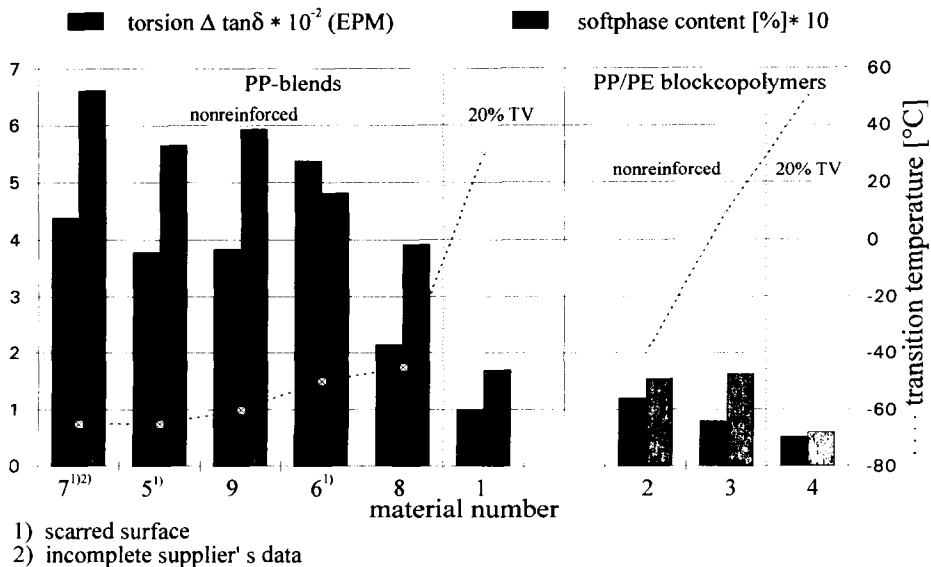


Fig. 8. Tough/brittle transition temperatures evaluated by the instrumented puncture test in comparison to the $\Delta \tan \delta$ peak values and to the content of the EPM component.

3. Rubber composites

Today, rubber composites are considered high-performance materials that are used for a variety of industrial applications. A comfortable climate in the interior of a car, irrespective of the time of year or kind of weather, is only possible with air conditioning. In Europe, the number of cars equipped with air conditioning has steadily risen in recent years. Depending on the car model, between approx. 30%, e.g. Mercedes-Benz middle class, and approx. 90%, e.g. Mercedes-Benz S-class, of cars are provided with air conditioning [18]. Flexible hose connections are indispensable for the compensation of the relative movements of the units positioned between motor and body and for the necessary workability during installation. Apart from many other requirements, e.g. made with respect to the low temperature and heat pressure resistance, thermal expansion behaviour, the tensile and flexural rigidity or the bursting pressure, vibration (noise production) and impulse pressure behaviour, to name just a few [19], these hoses must be resistant and impermeable to the coolant employed so as to ensure reliable operation of the unit and protection of the environment. Due to its ozone-depleting potential (ODP), difluorodichloromethane (R 12) used in the past, had to be substituted by the chlorine-free trifluorofluoroethane (R 134a). Since this coolant possesses a global warming potential (GWP), however, new coolant hoses which prevent coolant diffusion into the environment had to be developed. This problem can only be solved by a multilayer hose construction.

Because of this new coolant, a new material evaluation had to be made to ensure that, among other demands [19], no moisture could penetrate into the coolant circulation, which would not only lead to corrosion damage of the air-conditioning device but also to frosting-up in the thermostatic expansion valve in particular. The water (vapour) permeability was investigated by a device developed by the German Institute for Rubber Technology in Hannover. The quantitative determination of the penetrated water was effected by gas chromatography through measurement of the acetylene, which is produced quantitatively and stoichiometrically from water and calcium carbide. Four commercially available hoses were tested. Their details are described in Table 8. Fig. 9 displays the results. Hoses 1 and 4 were the best by far, which was to be expected on account of the butyl rubber layer. The bad result of Hose 3 came as

Table 8
Investigated hose designs

	Hose no. 1	Hose no. 2	Hose no. 3	Hose no. 4
Thermoplastic barrier film	PA 6 + 12 impact modified	PA 6	PA 6	PA 6 + 12
Elastomeric inner layer	IIR	NBR	HNBR	IIR
Elastomeric middle layer	IIR	none	none	none
Fabric	Polyester	Rayon	Aramid	Polyester
Elastomeric outer layer	EPDM	CR	HNBR	EPDM

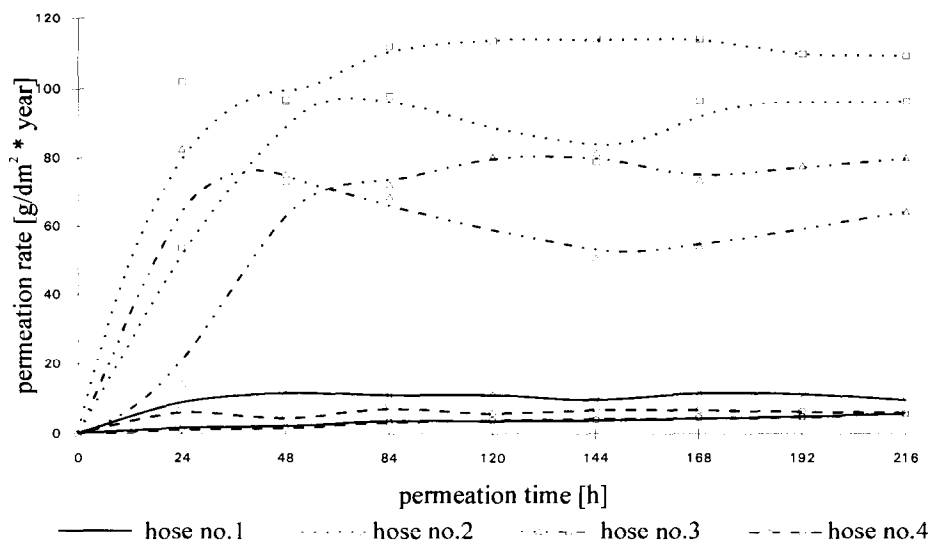


Fig. 9. Water (vapour) permeation rates through coolant hoses of air-conditioning devices at 70°C versus time.

a surprise, since it was assumed that the relatively expensive hydrogenated nitrile rubber (HNBR) would be a very good barrier against moisture.

To gain further insights into the changes in mechanical properties, especially those dynamic mechanical properties which determine the vibration and noise production behaviour, DMA spectra were run with the best (hose no. 4) and the worst (hose no. 2) hose after they had been subjected to the water (vapour) permeability testing device to 100% moisture in a waterbath of 70°C for 9 days (216 h).

Decisive for a good noise reduction behaviour is that almost no changes occur in the operating temperature range between -30 and 150°C . Looking at the characteristic peaks in the $\tan \delta$ curve (Table 9) for the best (no. 4) and the worst (no. 2) hose, it becomes clear that hose no. 4 meets this prerequisite. An important fact also seems to be that there are no changes in the $\tan \delta$ values of hose no. 4 within the entire operating temperature range from -30 to $+150^{\circ}\text{C}$, whereas this is only true above 0°C for hose no. 2. At this temperature, however, hose no. 2 has a $\tan \delta$ value of 0.2 which is better than that of hose no. 4 ($\tan \delta = 0.1$ at 0°C). As the temperature increases, their values assimilate. This leads to the conclusion that hose no. 4, after being in service for a prolonged period of time, shows less noise production in winter in the cold start phase of a car than hose no. 2.

Using IR spectroscopy, no significant changes could be found.

4. Recycling

Finally, the subject of recycling has to be addressed. When discussing the recycling of polymer materials, one has to distinguish between three large groups: the material, the raw material or chemical, and the energetic or thermal recycling. With a few exceptions

Table 9
Hose design and DMA results

	Hose no. 2	Thickness/mm	Hose no. 4	Thickness/mm
Thermoplastic barrier film	PA 6	0.1	PA6 + 66	0.4
Elastomeric inner layer	NBR	2.2	IIR	1.2
Fabric	Rayon	1	Polyester	1
Elastomeric outer layer	CR	1.3	EPDM	2.2
	T_g °C		tan δ	
	Virgin	After permeation test	Virgin	After permeation test
Hose no. 2				
NBR layer	-44.0	-39.2+/-0.4	0.37	0.40+/-0.02
CR layer	-26.0	-21.4+/-0.3	0.41	0.35+/-0.01
Hose no. 4				
IIR/EPDM layer	-52.5	-51.0+/-0	0.43	0.46±/-0.02
PA6/PA12 film	26.3	34.5+/-1.1	0.20	0.17+/-0

the material recycling dominates in industrial practice today and probably in the foreseeable future. For this reason only this aspect will be treated here.

4.1. SMC (sheet moulding compound) scrap for reinforcement of PA 66

About 30% SMC was simply added without further pretreatment to polyamide. DMA measurements showed that only the onset temperature (the beginning of the glass transition range) of the storage modulus increased slightly to higher temperatures (8.2–12.4°C). However, storage modulus below the glass transition range, 5.5 GPa for the SMC/PA compound compared to 4.4 GPa, is on a distinctly higher level. At 1.5 GPa, as compared to 1.0 GPa, the average value above the glass transition range is also much higher. However, for temperatures up to about 120°C, the toughness, characterized by the mechanical loss factor tan δ , is as much as 50% lower. This changes at higher service temperatures.

4.2. Recycling of pure-grade thermoplastic production scrap

This subject is actually state of the art in the plastics processing industry and is thus, solved if only a certain percentage of production scrap that has been processed several times is added to virgin material. For high performance and therefore very expensive thermoplastics like fluoroplastics, it is important to know whether it is possible to use 100% regrind without further compounding.

Two fluoroplastics were investigated, a tetrafluoroethylene/ethylene-copolymer (ETFE) from Du Pont (trade name Tefzel 280 MFR) and a polyvinylidene fluoride (PVDF) from Hüls Troisdorf AG (trade name Dyflor 2000). Their price per kilo is about 80 DM, which means that the use of 100% regrind would be highly significant from the economical point of view. Because of their superb resistance to even highly aggressive liquids, which is a prerequisite for bottle dispenser heads for dosing such aggressive liquids in laboratories, fluoroplastics are used worldwide. In 1992 the firm Brand, Wertheim, sold 60,000 of its dispensettes[®] and the trend is still rising. In these dispensers, the core, the dispensette head as well as two valves are made of ETFE, the cannula-holding device for the output cannula is made of PVDF, and the suction pipe is made of tetrafluoroethylene/hexafluoropropylene-copolymer (FEP) [20].

ETFE and PVDF samples for tensile testing as well as finished parts like dispensette heads were produced on a Klöckner Ferromatik Desma FX50 microprocessor-controlled injection-moulding machine. The material was thus processed once. Some of these test pieces were ground again and parts were injection-moulded once more from 100% of this regrind (2nd processing). The same procedure took place with some of these parts (3rd processing). After each processing stage, tensile testing samples were immersed for 30 days in standard laboratory chemicals such as toluene, tetrahy-

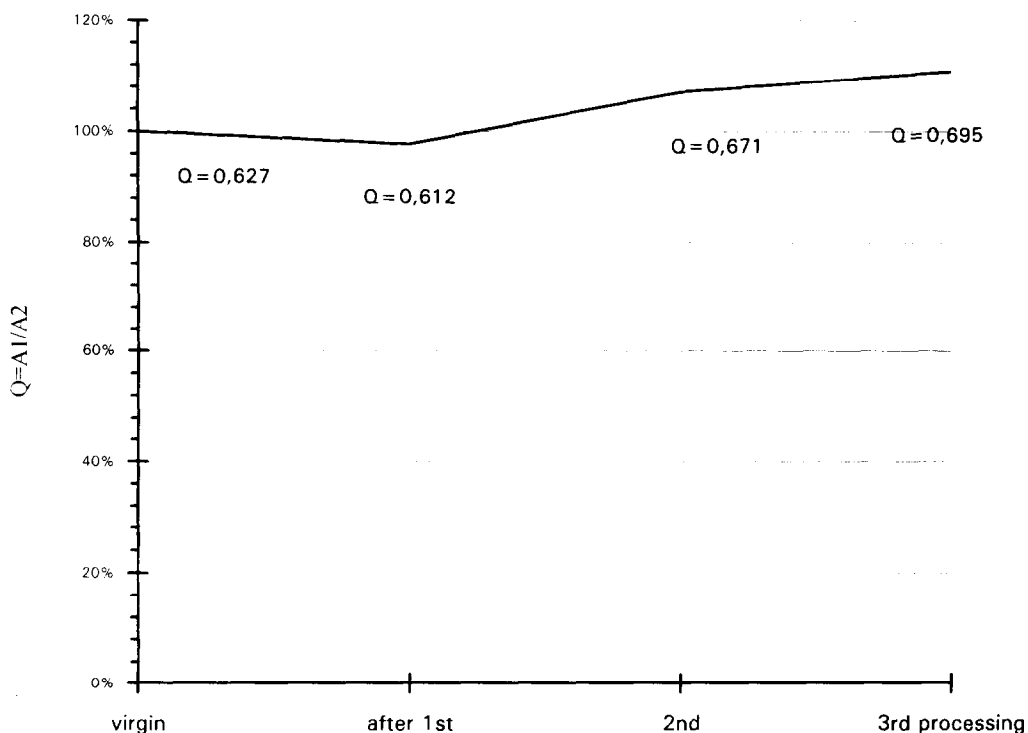


Fig. 10. Injection-moulded dispenser heads made of Tefzel 280 MFR: IR absorption quotient $Q = A_1$ (667 cm^{-1})/ A_2 (509 cm^{-1}) versus number of processings.

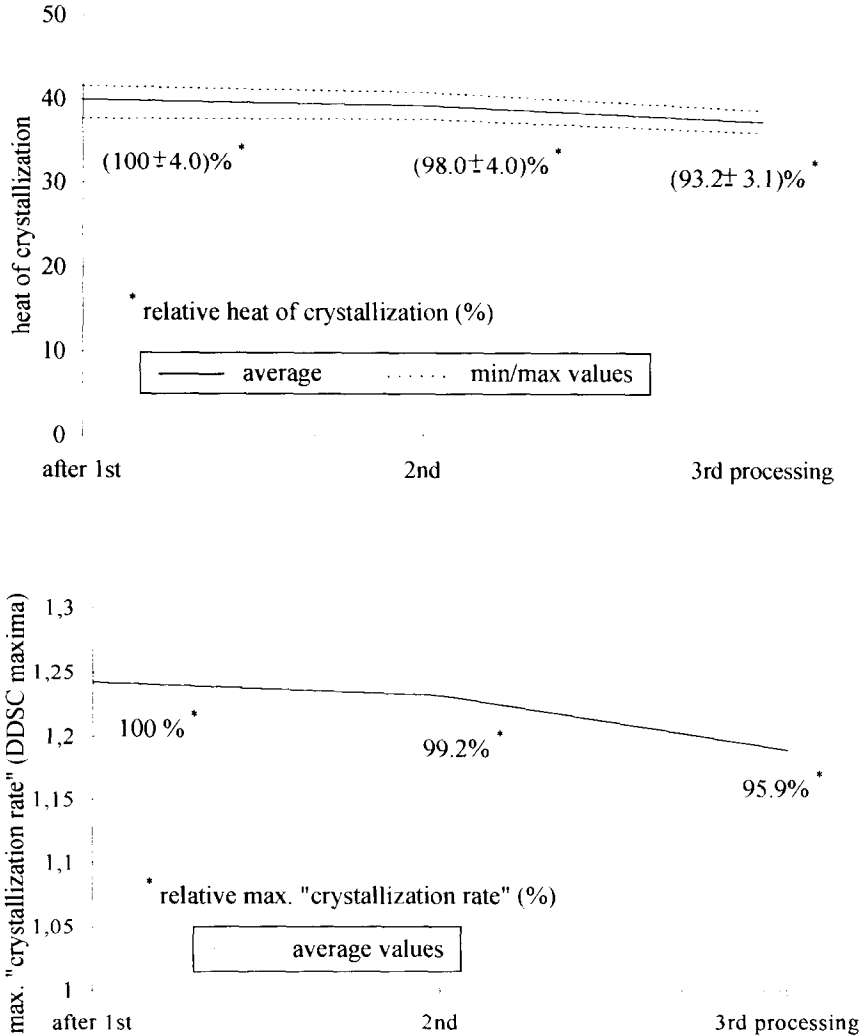


Fig. 11. Injection-moulded dispenser heads made of Tefzel 280 MFR: crystallization heat and maximum of the "crystallization rate" measured by DSC versus number of processings.

dofuran, acetone and concentrated hydrochloric acid. Then tensile strength, DSC and IR measurements were made. In the following, only ETFE will be discussed, because PVDF showed similar results. In addition, to tensile strength the crystallization temperature and the maximum rate of crystallization (maximum of the 1st derivative of the DSC signal in the crystallization zone), and the ratio of IR absorptions at 667 and 509 cm^{-1} , which indicates the changes on the CF^2 groups of the molecule, proved to be significant values.

The crystallization was selected for the simple reason that it characterizes possible changes in the crystallization behaviour during injection moulding. If the DSC and IR investigations are examined, it can be seen that, within the measurement accuracy, no changes are displayed if the material has only been processed once (Figs. 10 and 11). Only after the material has been processed twice do slight changes of 7% occur in IR spectroscopy, which increases to 11% after the third processing (Fig. 10). Also only very small changes (max. 7%) could be found by DSC (Fig. 11). This is also verified by the tensile strength, even after immersion in chemicals (Fig. 12). No significant influence of the different chemicals was observed, so the conclusion is that 100% regrind from material processed twice can be used for a 3rd processing without problems.

4.3. Identification of plastics after 10 years aging (service life)

As far as quantity is concerned, this problem is surely of greater importance than the recycling of pure grade production scrap. One just has to think of the 14 million old cars in Western Europe or the 2.3 million in West Germany which were scrapped in 1991 [21]. The average service life of cars in Germany is 12 years. Therefore the surface of exterior automobile parts will be degraded by environmental influences to such a degree that it is no longer possible to identify plastics by IR spectroscopy without sample preparation. There are tests, however, in which if quick removal of the surface with a knife is sufficient to expose enough basic material, IR spectroscopy becomes possible [22]. Another method just as quick as IR spectroscopy but which does not make it necessary to remove the surface is photoacoustic spectroscopy (PAS) [23].

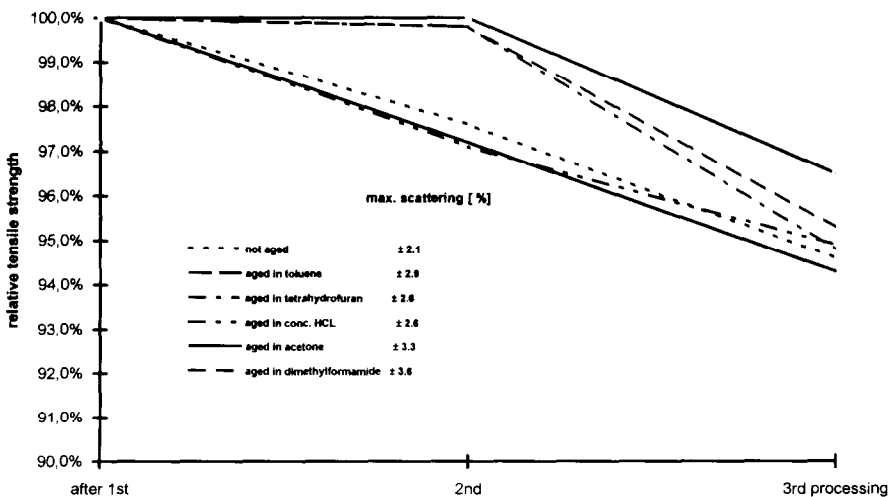


Fig. 12. Injection-moulded shoulder rods made of Tefzel 280 MFR: tensile strength after 30 days.

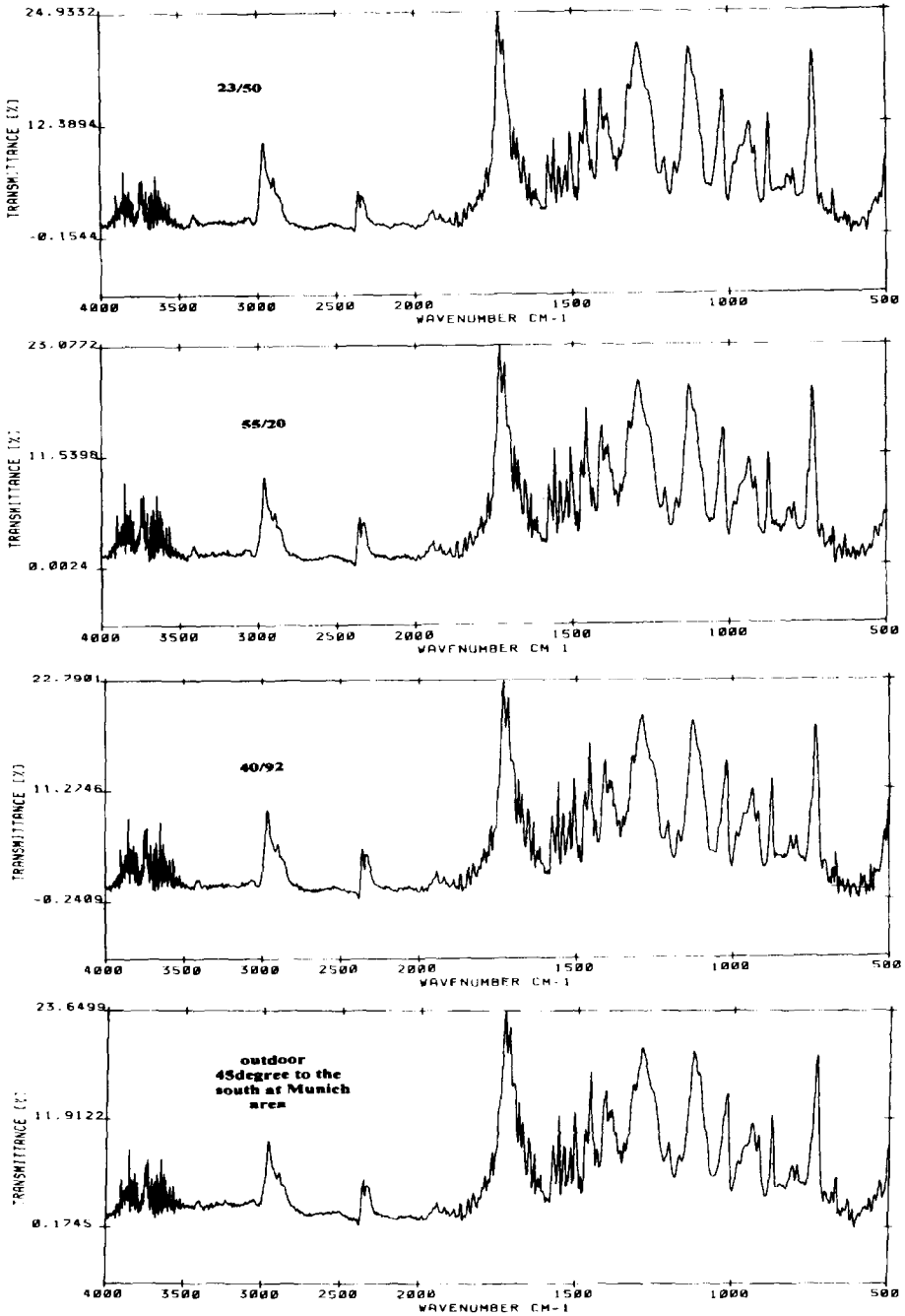


Fig. 13. Photoacoustic spectrum of polybutyleneterephthalate after ten years aging under four different conditions.

By selection of the appropriate modulation frequencies, it is possible to receive acoustic signals (heat waves) from different depths of the test piece from IR radiation absorbed by the sample. The quality of the spectra received is even better if the surface is structured, as in the case of foam, for example. A PA 66 (trade name, Ultramid A3K from BASF), a polycarbonate PC (trade name, Makrolon 2800 from Bayer AG) and a PBT (trade name, Ultradur B 4500 from BASF; Fig. 13 shows the PAS spectra) were measured after they had been stored for 10 years at 23°C and 50% relative humidity, at 55°C and 20% relative humidity, at 40°C and 92% relative humidity, or outdoor weathering at an angle of 45° in southerly direction in the area of Munich.

Acknowledgements

I would like to thank all the students who have written diploma theses as well as their partners in industry mentioned in the bibliographical references, the company Netzsch-Gerätebau, Selb/Germany, for having made available numerous thermoanalytical measurements and especially Dr. J. Opfermann of Netzsch for numerous discussions regarding the reaction-kinetic evaluations.

References

- [1] M. Schweizer, Evaluation of kinetic parameters of EP resin systems used in the aircraft and aerospace industry, Diploma thesis at the Department of Plastics and Rubber Engineering of Polytechnic (Fachhochschule) of Wuerzburg in collaboration with DASA (Dept. ZTT54), Munich, 1992.
- [2] J. Opfermann, G. Wilke, J. Jung, W. Ludwig, S. Hagen, M. Gebhardt and E. Kaisersberger, Global Analysis of Thermokinetics—a step towards invariant kinetic parameters and high distinguishness of the models used, in H.J. Flammersheim (Ed.), *Thermoanalytical Methods in Industry and Research*, 6th Autumn Meeting, Meisdorf, 1988.
- [3] J. Opfermann, Netzsch Thermokinetic Analysis, MultipleScan, Netzsch-Geraetebau GmbH, Selb/Germany, 1991.
- [4] ASTM E 698, Arrhenius Kinetic Constants for Thermally Unstable Materials, 1979.
- [5] J.F. Carpenter, Physicochemical testing of altered composition 3501-6 epoxy resin; 24th National SAMPE Symposium.
- [6] NN: Fibredux 914, High temperature resistant unidirectional prepregs, Bonded Structures, Ciba-Geigy Plastics Duxford Cambridge, UK, Information sheet No. FTA49F, October 1989.
- [7] ASTM D 2733, Interlaminar Shear Strength of Structural Reinforced Plastics at Elevated Temperatures, 1970.
- [8] H.J. Flammersheim, N. Eckhardt and J. Opfermann, The step growth polymerization of dithiols and diisocyanates. Part 1: DSC and spectroscopic investigations regarding the mechanism, *Thermochim. Acta*, 229 (1993) 281–287.
- [9] M. Schemme, L. Hofmann and G.W. Ehrenstein, Quality assurance during processing of fiber reinforced plastics, from BMFT-status symposium "Support program fiber reinforced materials". Look back, results and future, Braunschweig, 15./16.6.1994, S.85-103.
- [10] NN: Vicotex M 18, High Temperature and Damage Tolerant 180°C Epoxy Resin, Preliminary Data Sheet N°R 1300/June 1991-Issue 1 from Brochier SA, Neuilly-sur-Seine/Paris-France.
- [11] J. Reininger, Thermal expansion behaviour of carbon fiber reinforced plastics especially in the glass transition range—Application of dilatometry for the determination of the glass transition temperature, Diploma thesis at the Department of Plastics and Rubber Engineering of Polytechnic (Fachhoch-

- schule) of Wuerzburg in collaboration with Military Science Institute for Material Testing, Erding/Germany, 1986.
- [12] J. Seubert, Application possibilities of instrumental analysis and simple laboratory methods for the quantitative determination of triallylisocyanurate (TAIC) in uncrosslinked and radiation crosslinked flame-retarded glass fiber reinforced polyamide 66, Diploma thesis at the Department of Plastics and Rubber Engineering of Polytechnic (Fachhochschule) of Wuerzburg in collaboration with Siemens AG, Amberg/Germany, 1991.
- [13] H.D. Bickel, in *Fundamentals and Application of Radiation Crosslinkage*, VDI Publishing House, Düsseldorf, 1985, p. 215 onwards.
- [14] B. Kelm, Effort to establish a correlation between the dynamic-mechanical thermal analysis and the instrumented puncture test on impact modified thermoplastics, Diploma thesis at the Department of Plastics and Rubber Engineering of Polytechnic (Fachhochschule) of Wuerzburg in collaboration with Adam Opel AG, TEZ-central laboratory, Rüsselsheim/Germany, 1994.
- [15] S. Haftka and K. Könneke, Hoechst AG Frankfurt/Main, personal information.
- [16] P. Frey, Anisotropic expansion behaviour of injection moulded LCP-blends, Diploma thesis at the Department of Plastics and Rubber Engineering of Polytechnic (Fachhochschule) of Wuerzburg in collaboration with Siemens AG (Department ZFE ME AC 22), Erlangen, 1990.
- [17] A. Warmuth, Improvement of heat resistance of thermoplastic polyurethane through modification of other polymer materials, Diploma thesis at the Department of Plastics and Rubber Engineering of Polytechnic (Fachhochschule) of Wuerzburg in collaboration with Bayer AG, Department Rubber Application Technology, Leverkusen, 1989.
- [18] K.-H. Stump, Water (vapour) diffusion behaviour of coolant hoses for automobile air conditioning with special regard to the new coolant R 134a, Diploma thesis at the Department of Plastics and Rubber Engineering of Polytechnic (Fachhochschule) of Wuerzburg in collaboration with Mercedes-Benz AG (Dept. VWT), Sindelfingen, 1993.
- [19] NN., Coolant hoses for automobile air conditioning; information brochure of Mercedes-Benz AG, and DBL 6228 (Daimler-Benz delivery regulations), Application profile of coolant hoses at air conditioning devices.
- [20] M. Schreiber, Recycling of plastics—Changes in properties of fluoroplastics effected by the use of regrind, Diploma thesis at the Department of Plastics and Rubber Engineering of Polytechnic (Fachhochschule) of Wuerzburg in collaboration with Brand GmbH & Co., factory for laboratory equipment, Wertheim, 1993.
- [21] P. Zumbroich and B. Kiefer, Status report on scrap car utilization and government regulations, topical report VDA/PRAVDA and on the state of car-recycling at Adam Opel AG, in *Plastics in the Automobile Industry: Raw Materials, Building Components, Systems*, VDI Publishing House, Düsseldorf, p. 232–246.
- [22] D.F. Gentle, Automatic Identification of Plastics taken from End of Life Vehicles, in *Plastics in the Automobile Industry: Raw Materials, Structural Components, Systems*, VDI Publishing House, Düsseldorf, 1994.
- [23] S. Rahner, Photoacoustical Fourier-transform-infrared-spectroscopy in comparison to conventional methods with the example of polymer materials, Diploma thesis at the Department of Plastics and Rubber Engineering of Polytechnic (Fachhochschule) of Wuerzburg in collaboration with Siemens AG (Dept. ZPL 1 TW 45), Munich, 1993.